Lifetime measurements in ^{71}Ge and a new interacting boson-fermion model interpretation

M. Ivaşcu, N. Mărginean, D. Bucurescu, I. Căta-Danil, and C. A. Ur
Horia Hulubei National Institute of Physics and Nuclear Engineering, Bucharest, Romania

Yu. N. Lobach
Institute for Nuclear Research, pr. Nauki 47, 252028 Kiev, Ukraine
(Received 21 December 1998; published 30 June 1999)

The lifetimes of twelve low spin excited states have been measured in ^{71}Ge using the Doppler shift attenuation method in the ^{71}Ga$(p,n\gamma)$ reaction at 3.0 and 3.5 MeV incident energy. New interacting boson-fermion model calculations for this nucleus account well for the properties of all its levels known up to about 1.5 MeV excitation. [S0556-2813(99)03807-8]

PACS number(s): 21.10.Tg, 21.60.Fw, 23.20.Lv, 27.50.+e

I. INTRODUCTION

The nuclei with mass $A \approx 70$ belong to an interesting transitional region, with properties which vary rapidly with Z or N. The capacity of different nuclear models used to describe such nuclei is much better assessed if a reasonable large number of spectroscopic properties (energy levels and their decay properties) are available experimentally.

The ^{71}Ge nucleus, with $N=39$, lies in the middle of the 28 to 50 neutron shell. Its low spin and excitation energy properties (up to about 1.7 MeV excitation) are rather well determined, from the point of view of level position, spin-parity values, and electromagnetic decay branching ratios. This is the combined result of many experimental studies, including β decay [1,2], $(\alpha,n\gamma)$ reaction [3–5], $(p,n\gamma)$ reaction [6,7], as well as the neutron transfer (p,d) [8] and (d,p) reaction studies [9] (for other earlier works see Ref. [10]). However, the experimental information concerning the lifetimes of excited states in this nucleus (therefore, on absolute electromagnetic decay rates) is extremely limited: lifetimes are known only for the isomeric states $5/2_1^-$ at $E_x = 174.9$ keV and $9/2_1^+$ at $E_x = 198.4$ MeV [10], and for four other medium spin levels, as determined from a Doppler shift attenuation (DSA) measurement in the $(\alpha,n\gamma)$ reaction [4].

The level structure of ^{71}Ge has been recently discussed within the frame of the interacting boson-fermion model-1 (IBFM-1) [11] in Refs. [1,2], and of the dynamical collective model [6]. Due to the relatively poor knowledge of the decay properties (especially lifetimes) the comparison between the theoretical calculations and experimental data is not too detailed and leaves ambiguities. In particular, it has been suggested [1,2] that some of the low-lying levels have an ''intruder'' character (that is, they probably result from two-particle–two-hole excitations of the core, and thus do not belong to the IBFM space), therefore a more detailed study of their properties is of considerable interest.

In this work we present the first extensive lifetime measurements for excited states in ^{71}Ge, using the DSA method in a $(p,n\gamma)$ reaction. Given the scarcity of such data in this nucleus, the use of such a nonselective reaction is expected to lead to a better characterization of many low-lying, low-spin levels, and thus offer a rich ground for comparison with theoretical calculations. We were therefore able to reinvestigate the structure of ^{71}Ge in terms of the IBFM, based on the whole experimental information available at present. The next two sections present the experimental method and the results. Section IV presents IBFM calculations and their comparison with experimental data and Sec. V the conclusions of this work.

II. EXPERIMENTAL METHOD

The ^{71}Ge levels were populated via the ^{71}Ga$(p,n\gamma)$ reaction at two incident energies of 3.0 and 3.5 MeV, respectively. The proton beams, with intensities kept between 10 and 20 nA, were provided by the FN tandem Van de Graaff accelerator in Bucharest.

The target was a Ga pellet, isotopically enriched to 99.6%, of thickness 20–30 mg/cm^2, sticked onto a 0.1 mm thick Ta backing. The Ta backing was mounted on a finger cooled by air circulated in the upper part of a Dewar with liquid nitrogen, thus maintaining the target at a temperature of almost 0 °C. γ rays were detected in two 20% efficiency HPGe detectors with full width at half maximum (FWHM) energy resolutions of 2.0 and 2.2 keV at 1.33 MeV, respectively, placed at 13 cm from the target. Singles spectra were recorded simultaneously with both detectors at eight different angles from 0° to 143° with respect to the beam axis, choosing for each detector a random order of the angle sequence.

A continuous monitoring of the energy calibration was performed by measuring between runs a set of ^{60}Co, ^{137}Cs, and ^{152}Eu sources. The ^{60}Co source was also kept in a convenable position near the reaction chamber during all measurements. Since the (p,n) reaction at our energies provides very low recoil velocities, the DSA method, based in this case on the observation of the peak centroid shift with the angle, requires a very precise energy calibration. Thus, for the final analysis we kept only the spectra which presented gain shifts smaller than the typical imprecission in the determination of the peak centroids.

The proton incident energies resulted as a compromise between the requirement of being close to the threshold energies of the levels up to about $E_x = 2.0$ MeV (such that the

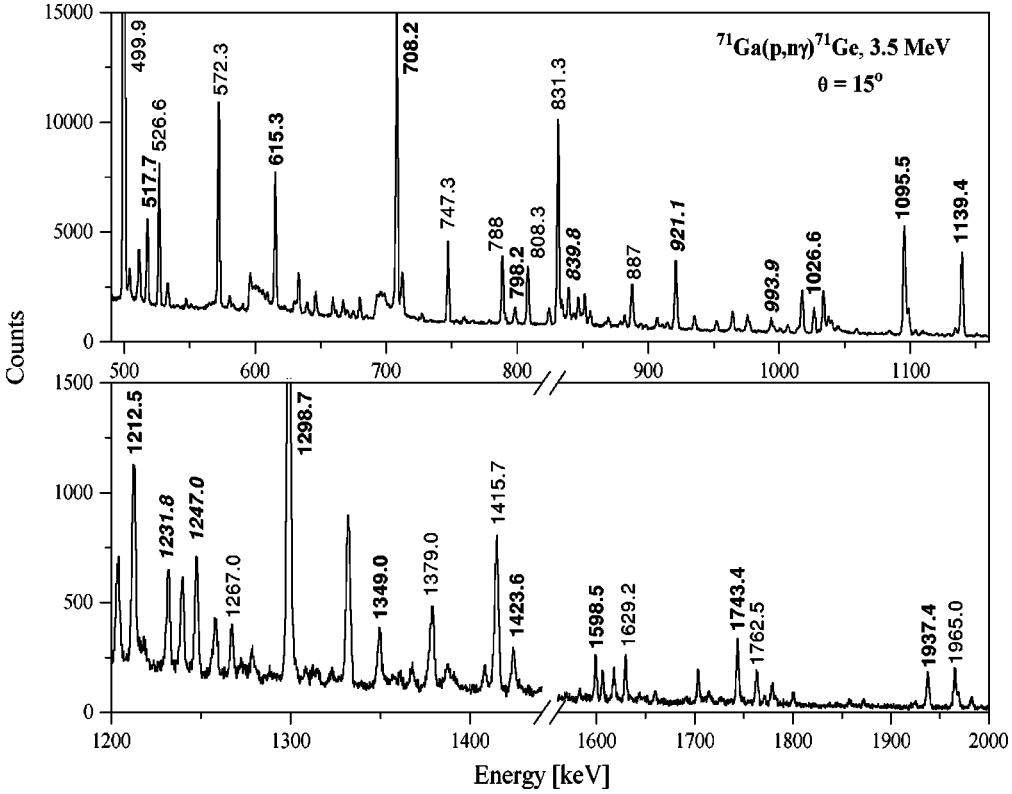

FIG. 1. Example of single γ-ray spectra obtained at 3.5 MeV proton incident energy and an angle of 15°. The most important transitions of ^{71}Ge are labeled with their energy in keV. Lifetime information could be extracted for the transitions labeled with bold numbers (see Table I and Fig. 2); for those labeled with bold italics, information concerning the mixing ratio could be extracted (Table II and Fig. 3).

recoils have a narrow velocity distribution close to the center of mass velocity), and that of having sufficient cross section for the levels of interest (in order to keep the measuring time for each angle reasonably short, up to 2–3 h, to prevent gain shifts of the electronic chain).

III. EXPERIMENTAL RESULTS

In two previous measurements we found out that all important γ rays from levels up to about 2.0 MeV in ^{71}Ge have rather small Doppler shifts, difficult to measure accurately. We succeeded, finally, with one experiment in which the stability of the detectors and associated electronics had the desired level.

Figure 1 shows an example of the measured γ-ray spectra. The calibration spectra taken with the standard sources between the runs at different angles have shown a good stability, therefore the initial calibration of the runs was made using these spectra. Some prompt γ rays clearly displayed Doppler shift effects, whereas others were found completely unshifted (corresponding to ''long'' lifetimes of their levels). In the final spectra analysis we have used some of the unshifted peaks (174.95, 326.79, 499.9, and 808.25 keV [10]), together with the 1173.24 keV peak of ^{60}Co (1332.50 keV formed a doublet with a line of ^{71}Ge) and the 1460.83 keV ^{40}K (background) line, to perform an internal energy calibration of each spectrum.

A. Lifetime determinations

Figure 2 shows examples of the observed variation of the γ-ray peak centroid energies with the observation angle, for ^{71}Ge transitions for each we could detect a Doppler shift. The straight lines are fits to the data with the usual DSA formula

$$E_\gamma = E_0\left(1 + F_{\exp}(\tau)\frac{\tilde{v}}{c}\cos\theta\right), \tag{1}$$

where E_0 is the unshifted γ-ray energy, $\tilde{v}$ is the mean initial velocity of the nuclei recoiling and being stopped into the target material, and $F_{\exp}(\tau)$ is the experimental attenuation factor. Since we are relatively close to the threshold energies, $\tilde{v}$ has been chosen as the center of mass velocity. Working close to the threshold ensures also that cascade feeding of the levels of interest is not important, and therefore $F_{\exp}$ will depend only on the lifetime τ of the level.

Table I centralizes the $F_{\exp}$ values extracted from various experimental runs. The γ-ray energies listed in this table are those from Refs. [1,10]. These values agree rather well with those that can be read from Fig. 2. A systematic disagreement, slightly increasing with the energy, occurs for the γ rays with the highest energies (1598.5, 1743.4, 1937.4 keV) which are underestimated in our case (1598.2, 1742.9, 1936.8 keV, respectively). This is due to our calibration curve whose highest point is at 1460.8 keV; nevertheless,

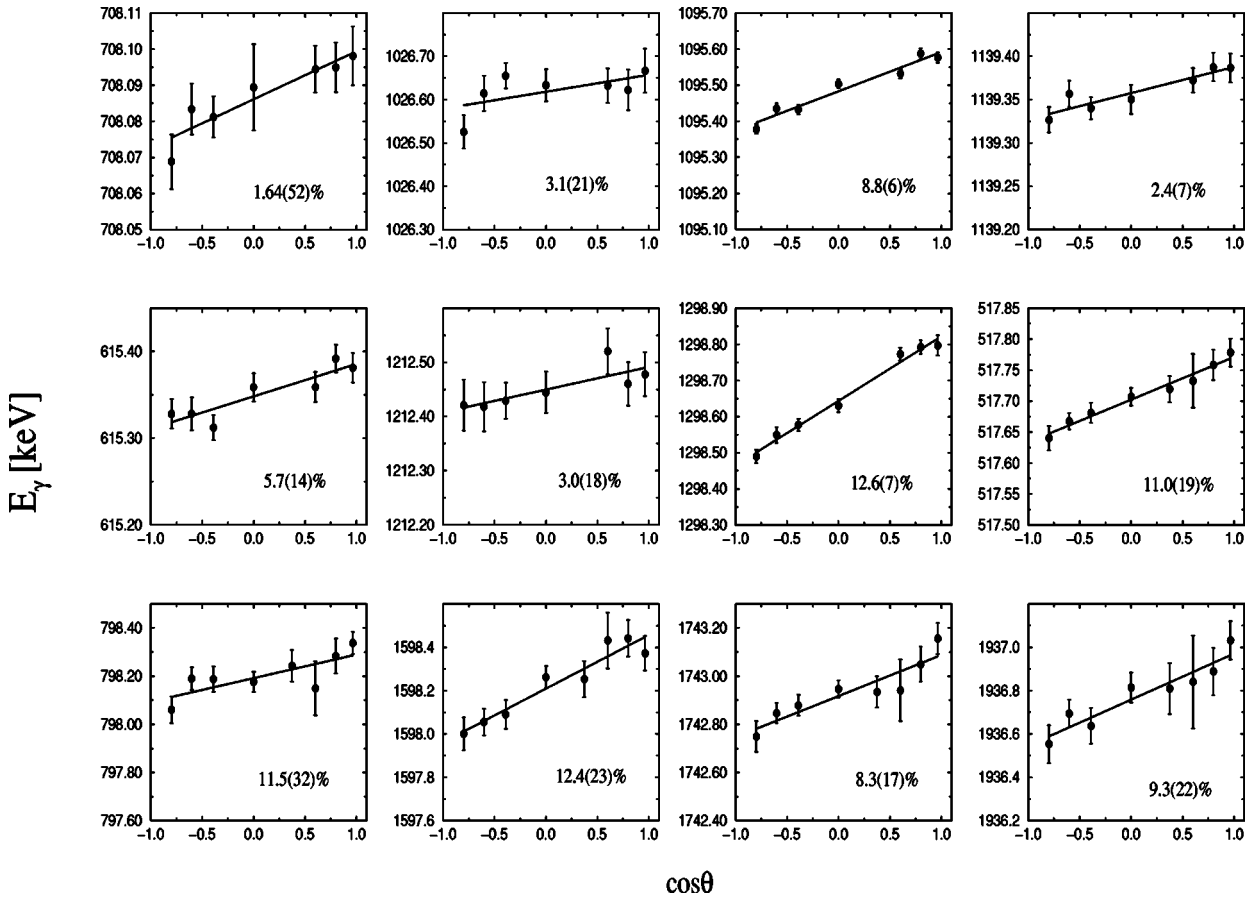

FIG. 2. Examples of attenuated Doppler shifts measured for γ-ray transitions in ^{71}Ge. The straight lines are fits to the data with Eq. (1), resulting in the $F_{\rm exp}$ values indicated for each transition. The characteristics of the run represented in each of the panels can be easily found by identifying the γ-ray energy and the $F(\tau)$ values in Table I (which summarizes all the measurements).

this procedure does not affect the relative energies at different angles, which are of main interest in deducing the $F(\tau)$ values. In general, more than one value could be determined for one given level. ''Missing'' runs in Table I indicate insuficient accuracy of the centroid determinations; for example the run at 3.5 MeV with detector 1 was not sufficiently stable. From Table I one can see that when more $F(\tau)$ values have been determined for a certain deexciting initial level these values are, generally, consistent with each other within the experimental errors. There is also no systematic variation of the F values with the incident beam energy, which indicates that there is no important cascade feeding of the levels of interest. To make this point clearer, Fig. 3 shows the level scheme of ^{71}Ge which is relevant fo the present lifetime measurements. From this figure, as well as from Fig. 1, one can see that the levels considered in the present experiment have rather unimportant cascade feeding, with the exception of the 708.2 keV levels, which will be discussed below.

Level lifetimes were determined from the $F_{\rm exp}$ values of Table I by comparing them with calculated $F(\tau)$ curves. We have used theoretical stopping powers in the calculations: the nuclear and electronic stopping powers have been treated according to the formalisms of Lindhard-Scharff-Schiott (LSS) [12] and Blaugrund [13]. Usually, these electronic and nuclear stopping powers are weighted by two factors f_e and f_n, respectively, which are determined empirically; these factors may vary considerably with the combination recoiling nucleus-stopping medium. In our case we have used the values $f_e=0.75$ and $f_n=0.55$ determined in a relatively low energy experiment [^{66}Zn$(\alpha,n\gamma)$ reaction at 13.5 MeV] [14], for a recoil-target combination very close to ours: Ge in Zn. The lifetimes resulted by using this stopping power are a factor of about 2 larger than those obtained from the use of the ''pure'' LSS stopping power ($f_e=f_n=1.0$). In other similar low-recoil DSAM lifetime measurements [18] we have found that using for the electronic stopping power the formalism of Ziegler *et al.* [16] leads to lifetimes 10 to 20 % higher than the LSS ones.

The procedure of extracting lifetimes from the $F(\tau)$ curve usually provides asymmetric errors. We have symmetrized the resulting errors according to the procedure outlined in Ref. [15]. When more values of τ were available the final adopted value (last column in Table I) is their weighted average. The final error in the lifetime contains also a 20% error added quadratically, to account for uncertainties in the calculated stopping powers. As discussed above, the $E_x=708.2$ keV level, which has the smallest measured $F(\tau)$ value (Table I), has the most important feeding from higher levels, especially from the 1506.4 keV one. Its effective

TABLE I. Summary of lifetimes measured in ^{71}Ge in the present work. The adopted lifetime values (last column) represent the weighted averages of the values extracted from the appropriate $F(\tau)$ values, and correspond to the LSS [12] stopping power with the coefficients $f_e=0.75$, $f_n=0.55$ (see text for other details). The final error in τ also contains (quadratically) a 20% error which accounts for uncertainties in the stopping power.

E_x (keV)	E_γ (keV)	Run identification E_i(MeV)/ detector nr.[a]	$F(\tau)$ (%)	τ (ps)
708.2	708.2	3.0/1	1.64(52)	<15.4
1026.6	1026.6	3.0/1	3.1(21)	>1.6
1095.5	1095.5	3.0/1	8.8(6)	0.90 ± 0.20
1139.4	1139.4	3.0/1	2.4(7)	5.7 ± 2.0
	1139.4	3.0/2	2.2(6)	
1205.1	615.3	3.0/1	5.7(14)	1.6 ± 0.4
	615.3	3.0/2	6.3(13)	
	615.3	3.5/2	5.5(11)	
1212.5	1212.5	3.0/1	3.0(18)	>1.7
1298.7	1298.7	3.0/1	12.6(8)	0.61 ± 0.13
	1298.7	3.0/2	11.6(7)	
	1298.7	3.5/2	13.3(7)	
1349.0	1349.0	3.0/1	11.4(33)	0.66 ± 0.16
	1349.0	3.0/2	15.9(34)	
	517.7	3.0/1	10.0(28)	
	517.7	3.0/2	9.6(25)	
	517.7	3.5/2	11.0(19)	
1506.4	798.2	3.0/1	15.1(66)	0.73 ± 0.23
	798.2	3.0/2	14.3(61)	
	798.2	3.5/2	11.5(32)	
1598.5	1598.5	3.0/1	8.0(37)	0.79 ± 0.21
	1598.5	3.0/2	9.9(54)	
	1598.5	3.5/2	12.4(23)	
	1423.6	3.0/1	10.5(55)	
	1423.6	3.5/2	9.9(33)	
1743.4	1743.4	3.0/1	15.4(45)	0.61 ± 0.21
	1743.4	3.0/2	15.7(43)	
	1743.4	3.5/2	8.3(17)	
1937.4	1937.4	3.5/2	9.3(22)	1.0 ± 0.4

[a]Incident proton energy and number of the detector.

$F(\tau)$ value, of 1.64 ± 0.52 %, leads to an effective lifetime of this level of $7.6^{+7.8}_{-2.6}$ ps. Due to the strong cascade feeding this lifetime is considered as an upper limit, therefore we give for this level $\tau<15.4$ ps.

B. Mixing ratio determinations

The determination of multipole mixing ratios of mixed transitions was not the original purpose of our measurements, but the data could be used to check existing values or try to complete them. Multipole mixing ratios (δ values) in this nucleus have been obtained mainly from three sources: the $(p,n\gamma)$ study [7], the $(\alpha,n\gamma)$ studies [4,5], and the ε-decay study of oriented nuclei [2]. With the exception of the most recent measurements [2] the results of all these works have been summarized, along with ''adopted'' δ values, in Ref. [10].

The $(p,n\gamma)$ reaction study [7], performed at incident energies up to 3 MeV, is similar to ours. They have analyzed the measured angular γ-ray angular distributions for different combinations of initial and final J^π values, by calculating the magnetic substate populations with the statistical model. Since the spin of the target nucleus is 3/2, the excited states with spin $\leqslant 3/2$ are expected to have little alignment, therefore their γ-ray angular distributions are practically isotropic. While for the transitions from $J=1/2$ states no δ values could be derived, for the $J=3/2$ states the extracted values have, usually, large errors [7]. With increasing spin, the alignment also increases, therefore the γ-ray angular distributions can provide δ values with an increased accuracy. As in Ref. [7] δ values have been proposed for most of the states with spin up to 5/2 and $E_x<1.3$ MeV, we have concentrated mainly on the states of higher spin (7/2 to 11/2) and energy above 1.3 MeV, which had mixed transitions with peaks well resolved in the spectra.

Angular distributions of the γ rays have been determined by normalizing the yields to that of the 808.3 keV transition $(1/2_2^- \rightarrow 1/2_1^-)$ which is expected to be isotropic. The determined a_2 and a_4 Legendre polynomial coefficients (with detector geometry correction taken into account) are given in Table II. For all transitions shown in Table II the initial and final J^π values are known. In order to determine the δ values we have used the formalism of Yamazaki [17] in which for the m-substate population of the initial state we made the simple assumption that it can be well approximated by a Gaussian of width σ. We have first treated both δ and σ as free parameters. The σ values thus extracted from different angular distributions, corresponding to the absolute χ^2 minima were in good agreement with each other and were well concentrated around the value $\sigma=2.24\pm0.12$ (their weighted average). We have therefore adopted this value as one which describes well the alignment in our (p,n) reaction, and determined δ values from the analysis of the usual plot χ^2 versus δ, using this value of σ. The results are given in Table II. One can see that the δ values thus determined agree very well, in several cases, with previous values determined from other measurements with comparable accuracy, which is an indication that this simple procedure provides correct mixing ratios for transitions from states with spin $J \geqslant 7/2$. One new δ value could be thus determined, in other cases the transition γ rays belonged to complex peaks thus making the analysis more uncertain.

IV. THEORETICAL INTERPRETATION

A first comparison of the experimental level scheme of ^{71}Ge with calculations based on the intermediate coupling

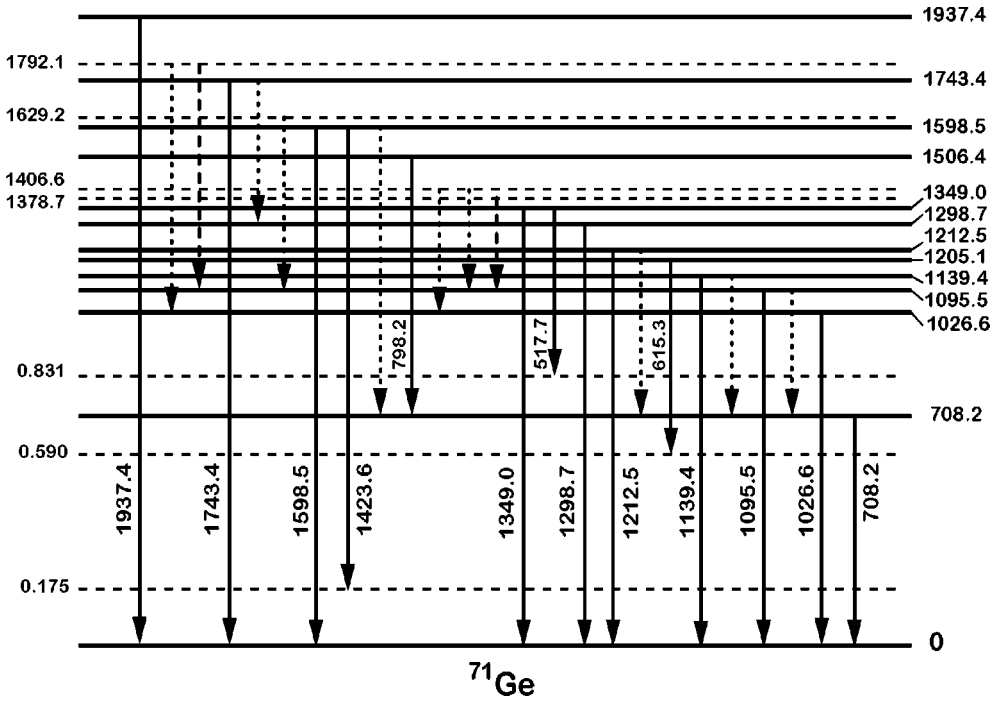

FIG. 3. Level scheme of ^{71}Ge, of relevance for the present lifetime measurements. This level scheme is very much simplified, showing only some levels and transitions. The following levels are given: (i) the levels from Table I, for which lifetimes have been derived in this work (drawn with heavy continuous lines) and (ii) other levels (see Ref. [10]) up to $E_x = 2.0$ MeV (drawn with dashed lines) which feed the levels from (i) or are fed by γ rays of interest. For all these levels, only the transitions for which $F(\tau)$ values have been determined (Table I) are shown, and also transitions which feed the levels of interest (i). These transitions are drawn: by a continuous line if the corresponding branching is larger than 10%, by a dashed line if it is between 5 and 10 %, and by a dotted line if it is below 5%.

model was made in Ref. [5]. Only a qualitative description of the first few negative parity levels was obtained, while the positive parity states were rather poorly described. More recently, in Ref. [6] a dynamical collective model was used. While the properties of some levels are reasonably well explained, a number of others have no theoretical counterpart; according to the authors, this is due to the fact that only the yrast levels of the core were taken into consideration in these calculations.

Interacting boson-fermion model (IBFM) calculations for this nucleus have been presented in two papers [1,2], both using the same parametrization of the Hamiltonian, in the IBFM-1 version of the model [11], which does not distinguish between neutrons and protons. Particular to this approach is that it treats some states in the ^{70}Ge core as ''intruder'' states (i.e., not belonging to the IBM space). The subsequent IBFM calculations did not account for two low-lying states, namely, $E_x = 831.3$ keV, $3/2^-$ and 1212.5 keV, $5/2^-$, which were consequently proposed as possibly resulting from coupling of the valence nucleon to the intruder excitations of the core nucleus. The comparison between experiment and calculations has been limited to the few absolute transition rates measured in Ref. [4], some branching ratios and known multipole mixing ratios [1,2].

The present work, in which lifetimes have been measured for a number of low-lying states provides new possibilities of a more detailed investigation of the IBFM predictions. To do this, we have used the whole presently available experimental information, including the level characteristics [10] with some recent updates concerning J^π values [6] and δ values [2], as well as the present lifetimes and the spectroscopic information from the neutron transfer reactions [8,9].

The IBFM calculations. As in the previous calculations [1,2] we have used the IBFM-1 version of this model [11]. The calculations were made with the codes ODDA (for levels), PBEM (for electromagnetic transitions) [19] and SPEC [20] (for one-nucleon transfer spectroscopic factors). ^{71}Ge is described as a fermion (neutron) coupled to a ^{70}Ge core.

(1) The ^{70}Ge *core*. We first described the ^{70}Ge core nucleus with the IBM-1 model [21], as a system of seven bosons. The model parameters have been determined such as to describe the known experimental data (level energies, branchings and B values). We have been working with the usual parametrization of the IBM-1 Hamiltonian (nonmultipole form): Eq. (1.35) of Ref. [22]. The adopted parameter values are $\varepsilon' = 1.088$, $c'_L(L=0,2,4) = -0.438$, -0.361, 0.090, $v_2 = 0.134$, $v_0 = -0.072$ (all in MeV) and have been determined with the following procedure. ε' is the energy of the d boson and is approximately equal to the $E(2_1^+)$ energy. In a first approximation ($v_0 = v_2 = 0$) the c'_L values are simply determined by the anharmonicities of the $0_2^+, 2_2^+, 4_1^+$ levels. Then, in order to reproduce the observed experimental $B(E2)$ ratios one needs to introduce the terms in v_0 and v_2 and slightly readjust the other parameters. The calculations have been performed with the code PHINT [24].

For the transition operators the parameters have been chosen as follows. The IBM-1 Hamiltonian described above can

TABLE II. Multipole mixing ratios $\delta(L+1/L)$ for transitions from some of the higher spin states in ^{71}Ge, as measured in the present experiment and compared to other existing values. a_2 and a_4 are the normalized Legendre polynomial coefficients (A_2/A_0 and A_4/A_0, respectively). The δ values correspond to a σ value (width of the Gaussian magnetic substate population) of 2.24 (see text for details).

E_x (keV)	J_i^π	J_f^π	E_γ (keV)	a_2	a_4	δ[a]	δ[b]
1038.2	$\frac{9}{2}^+$	$\frac{7}{2}^+$	448.4	0.225(71)	0.011(6)	+0.42(8)	+0.49(6)[c]
		$\frac{9}{2}^+$	839.8	0.256(71)	0.0000(1)	+0.10(18)	$+0.4^{+0.1}_{-0.3}$[c]
1096.0	$\frac{7}{2}^-$	$\frac{5}{2}^-$	921.1	−0.214(45)	0.065(25)	−2.99(44) or −0.10(7)	$-1.96^{+0.30}_{-0.040}$[d] or $-0.23^{+0.07}_{-0.08}$
1192.3	$\frac{11}{2}^+$	$\frac{9}{2}^+$	993.9	0.588(101)	0.117(61)	+1.26(50)	+1.3(5)[c]
1406.7	$\frac{7}{2}^-$	$\frac{5}{2}^-$	1231.8	0.233(63)	0.0096(54)	+0.58(15) or +3.15(44)	
1422.0	$\frac{9}{2}^-$	$\frac{5}{2}^-$	1247.0	0.313(115)	0.011(28)	+0.15(10) or +7.0(7)	−0.06(6)[c]

[a]Present values.
[b]Previous measurements.
[c]Adopted value (Ref. [10]).
[d]Reference [7].

also be transformed into an equivalent, multipole form: Eq. (1.53) of Ref. [22]. By doing this transformation we found for the quadrupole operator $\hat{Q}=(d^\dagger s+s^\dagger\tilde{d})+\chi(d^\dagger\tilde{d})^{(2)}$ a value χ which is close to the SU(3) limit $-\sqrt{7}/2$. Then, for the $E2$ transition operator we have used the same χ value, in the spirit of the extended consistent-Q formalism [25]. Recent results also show that large values of the parameter χ are needed for transitional and even vibrational nuclei [26].

A boson effective charge e_B (which normalizes the above quadrupole operator) of 0.064 e b ($E2SD$ in the notation of code FBEM [24]) has been determined by normalizing to the experimental $B(E2;2_1^+\rightarrow 0_1^+)$ value [23].

The lowest order $M1$ transition operator in the IBM-1 model is proportional to the angular momentum operator $\hat{L}$ and thus it does not produce $M1$ transitions. There are, nevertheless, several measured $M1$ transitions rates and $\delta(E2/M1)$ values [23]. In order to account for this, we have used the general second order $M1$ operator defined in Ref. [27]:

$$T(M1)=(g_b+AN)\hat{L}+B_1(\hat{Q}_1\hat{L})^{(1)}+B_2(\hat{Q}_2\hat{L})^{(1)}+C\hat{n}_d\hat{L}, \tag{2}$$

where $\hat{Q}_1$ and $\hat{Q}_2$ stand for the two parts of the $E2$ operator $(d^\dagger s+s^\dagger\tilde{d})$ and $(d^\dagger\tilde{d})^{(2)}$, respectively. The last term in Eq. (2) contributes only to $J\rightarrow J$ transitions. Previous investigations [27,28] have shown that, in general, one cannot have a proportionality between the sum of the two middle terms in Eq. (2) and the $E2$ transition operator. On the other hand, we had too little data to freely treat the B_1,B_2, and C parameters, so we actually used this restriction, although in this case the mixing ratios of transitions between different spins are completely independent of the detailed nature of the states, being determined only by the geometric properties of the operators [27]. For the parameters in the $M1$ operator above we have used the values (all in μ_N) $g_b=0.093$, $A=0$, $B_1=0.035$, $B_2=-0.047$.

With the $E2$ and $M1$ transition operators specified above, a reasonable description of the experimental $B(E2)$ values, magnetic moment of the 2_1^+ state and of the several $B(M1)$ and δ values, has been achieved (see below). Figure 4 shows the description of the level scheme of ^{70}Ge. Practically all states up to $E_x=3.0$ MeV, as well as the higher spin members of the yrast and quasi-γ bands are well described. It is notable that in this calculation we have described the 0_2^+ (1215 keV) and 2_2^+ (1708 keV) states as well, whereas these states have been considered intruders in the calculations of Refs. [1,2]. The present description is further validated by the reasonable reproduction of the γ-ray branching ratios and absolute transition rates, given in Table III. With the exception of the higher lying 2^+ states, which are well reproduced in position but whose branching ratios are not equally well reproduced, the other levels are generally well described. Thus, in the present calculations we found no need of considering the 0_2^+ and 2_2^+ states as intruders. The values specified above for the Hamiltonian and transition operators were subsequently used in the IBFM-1 calculations for ^{71}Ge.

(2) The ^{71}Ge nucleus. ^{71}Ge has been treated as a fermion coupled to the ^{70}Ge bosonic core. The IBFM-1 Hamiltonian employed in the present calculations has the general form [11]

$$H_{\mathrm{IBFM}}=H_{\mathrm{IBM}}+\sum_j E_j a_j^\dagger a_j+V_{BF}, \tag{3}$$

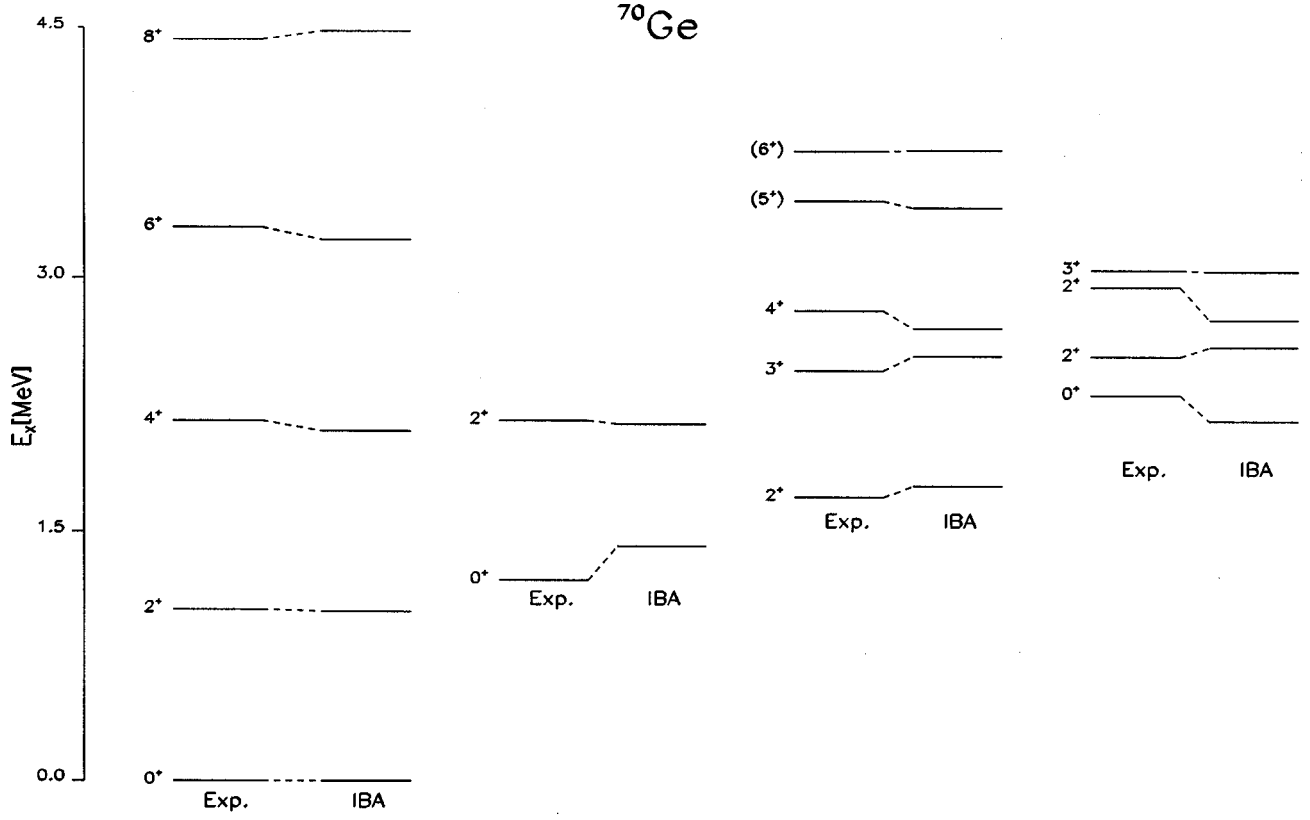

FIG. 4. Comparison between the experimental level scheme of ^{70}Ge and the one calculated with the IBM-1 model. Details concerning the static moments and the electromagnetic decay scheme are given in Table III. The model parameters are given in text.

where H_{IBM} is the IBM-1 Hamiltonian of the core (described above), the second term is the single quasiparticle energy term and V_{BF} is the interaction of the odd particle (fermion) with the bosons of the core. The main contributions to V_{BF} are [11] a monopole-monopole, quadrupole-quadrupole, and exchange interaction, for which we used a semimicroscopic parametrization [29]:

$$V_{mm} = -A_0 \sum_j \sqrt{5(2j+1)}\hat{n}_d \hat{n}_j , \tag{4}$$

$$V_{qq} = \sum_{jj'} \Gamma_{jj'} [\hat{Q}(a_j^\dagger \tilde{a}_{j'})^{(2)}]^{(0)}, \tag{5}$$

$$V_{\mathrm{exch}} = \sum_{jj'j''} \Lambda_{jj'}^{j''} : [(a_j^\dagger \tilde{d})^{(j'')} (d^\dagger \tilde{a}_{j'})^{(j'')}]^{(0)}, \tag{6}$$

where

$$\Gamma_{jj'} = \Gamma_0 \sqrt{5}(u_j u_{j'} - v_j v_{j'}) Q_{jj'} , \tag{7}$$

$$\Lambda_{jj'}^{j''} = \frac{-\sqrt{5}}{\sqrt{2j''+1}} \Lambda_0 [Q_{j'j''} \beta_{j''j} (u_{j'} v_{j''} + v_{j'} u_{j''}) + Q_{j''j} \beta_{j'j''} (u_{j''} v_j + v_{j''} u_j)], \tag{8}$$

$$\beta_{jj'} = \frac{(u_j v_{j'} + v_j u_{j'}) Q_{jj'}}{E_j + E_{j'} - \hbar\omega}, \quad Q_{jj'} = \langle j || Y_2 || j' \rangle . \tag{9}$$

For given quasiparticle energies E_j and occupancies u_j^2, the V_{BF} term is determined by the three strengths A_0, Γ_0, and Λ_0, respectively. The odd neutron was allowed to occupy the shell model orbitals between the magic numbers 20 and 50: $2p_{3/2}, 2p_{1/2}, 1f_{7/2}, 1f_{5/2}, 1g_{9/2}$, as well as $2d_{5/2}$ from the next shell. The quantities E_j, u_j^2 have been initially determined by a BCS calculation (with a standard pairing gap of $\Delta = 12A^{-1/2}$ MeV), starting from the spherical shell model single-particle energies of Reehal and Sorensen [30]. However, we have finally lowered the $2p_{3/2}, 2p_{1/2}$ doublet with 0.75 MeV with respect to the other states. The parameters A_0, Γ_0, Λ_0 were determined by repeatedly improving both the level scheme and the decay scheme description. A special mention is that in the BCS calculations we have explicitely considered the blocking of the unique parity orbital $1g_{9/2}$; the practical effect of the blocking is an increase in the occupation of this orbital. We have found, similarly to a previous investigation of the ^{73}As nucleus [18], that this procedure was essential in allowing the description of *both* negative and positive parity levels with the *same B-F* parameters (A_0, Γ_0, Λ_0), whereas in practically all cases reported in literature one accepts different (sometimes widely different) parameter values for the two sets of states. In our case we have used the values $\Gamma_0 = 0.39$ MeV and $\Lambda_0 = 2.14$ MeV^2, and only slightly different A_0 strength values (-0.20 MeV for negative parity and 0.06 MeV for positive parity states, respectively); the role of the monopole interaction is not, however, essential, as it leads only to a renormal-

TABLE III. Comparison between experimental and calculated (IBM-1 model) electromagnetic decay properties of states in ^{70}Ge. Calculated branching ratios smaller than 0.5 (relatively to a value of 100 for the strongest one) are not given unless the experimental ones exist. The last part of the table shows the known $\delta(E2/M1)$ values.

E_x (keV)	J_i^π	J_f^π	E_γ (keV)	$B(E2)$ (e^2 fm^4) expt.	$B(E2)$ (e^2 fm^4) calc.	$B(M1)$ (nm^2) expt.	$B(M1)$ (nm^2) calc.	Br. ratio expt.	Br. ratio calc.
1039.3	2_1^+	0_1^+	1039.3	360(7)	360			100	100
1215.4	0_2^+	2_1^+	176.1	823(51)	894			100	100
1707.9	2_2^+	0_1^+	1707.9	17(9)	9.8			85(1)	58
		2_1^+	668.6	1902(1028)	366	0.0045^{+55}_{-30}	0.047	100	100
		0_2^+	492.4	428(240)	327			4.6(1)	3.8
2153.5	4_1^+	2_1^+	1114.2	411(103)	693			100(1)	100
		2_2^+	445.6		182			0.8(2)	0.3
2157.4	2_3^+	0_1^+	2157.4		3.0×10^{-6}			12(2)	0.7
		2_1^+	1118.1		22.4		4.2×10^{-4}	100(10)	27.6
		0_2^+	942.0		231			44(5)	100
		2_2^+	449.5		442		0.070	3.3(8)	57.5
2306.9	0_3^+	2_1^+	1267.5	$>2.4(2)$	42			100(7)	100
		2_2^+	599.0	$>82(5)$	306			82(7)	17.1
2451.5	3_1^+	2_1^+	1412.2		5.6		3.9×10^{-4}	41(4)	25.3
		2_2^+	743.6		287	0.022(3)	0.020	100(1)	100
		4_1^+	298.0		52		6.9×10^{-3}	1.8(4)	1.5
		2_3^+	294.1		379		0.027	1	5.7
2535.7	2_4^+	0_1^+	2535.7		0.1				21.6
		2_1^+	1496.4		1.3		4.6×10^{-4}	100(11)	52.8
		0_2^+	1320.3		14.8			9.5(10)	100
		2_2^+	827.8		0.9		5.5×10^{-3}	23(5)	76.1
		2_3^+	378.3		180				40.6
2806.7	4_2^+	2_1^+	1767.4		32.7				88.8
		2_2^+	1098.8	497(206)	394			100(9)	100
		4_1^+	653.2		112		0.140	14(3)	89.7
		2_3^+	649.3		283				5.2
		3_1^+	355.2		230		0.031		3.3
2945.2	2_5^+	0_1^+	2945.2		1.3×10^{-6}				2.0
		2_1^+	1905.9		1.8×10^{-5}		2.0×10^{-4}		16.1
		0_2^+	1729.8		9.6				100
		2_2^+	1237.3		19.3		5.6×10^{-4}	100	48.2
		4_1^+	791.7		16.6				3.3
		2_3^+	787.8		1.3		0.020		93.0
		0_3^+	638.3		103				7.3
		3_1^+	493.7		41		2.9×10^{-3}		4.2
		2_4^+	409.5		382		0.022		17.8
3046.8	3_2^+	2_1^+	2007.5		2.6×10^{-5}		1.9×10^{-5}	18(2)	14.9
		2_2^+	1338.9		5.8		4.1×10^{-4}	54(6)	55.0
		4_1^+	893.3		2.0		2.6×10^{-4}	12(1)	5.4
		2_3^+	889.3		8.9		6.3×10^{-4}	19(2)	15.9
		3_1^+	595.3		2×10^{-16}		0.024	100(10)	100
		2_4^+	511.1		197		0.014		47.3
		4_2^+	240.1		9.8×10^{-5}		1.3×10^{-4}	1.3(2)	~0
		2_5^+	101.6		426		0.030		0.6
3297.3	6_1^+	4_1^+	1143.3	583(120)	967			100	100
		4_2^+	490.6		246				0.4

TABLE III. (*Continued.*)

E_x (keV)	J_i^π	J_f^π	E_γ (keV)	$B(E2)$ (e^2 fm^4) expt.	calc.	$B(M1)$ (nm^2) expt.	calc.	Br. ratio expt.	calc.
3753.4	6_2^+	4_1^+	1600.0		60			100	100
		4_2^+	946.7	463^{+205}_{-103}	586			100	70.5
		6_1^+	456.1		20.9		0.214		45.9
		5_1^+	297.4		211		0.066		4.0
4432.0	8_1^+	6_1^+	1134.7	737(377)	1094			100	100
		6_1^+	678.6		124				0.9

E_x (keV)	J_i^π	J_f^π	E_γ (keV)	$\delta_{\rm exp}$	$\delta_{\rm calc}$
1707.9	2_2^+	2_1^+	668.6	$-3.6^{+1.1}_{-0.6}$	-0.49
2451.5	3_1^+	2_1^+	1412.2	$-2.2^{+0.5}_{-0.3}$	-1.40
		2_2^+	743.6	$-0.05(8)$	-0.74
2535.7	2_4^+	2_1^+	1496.4	-0.75	-0.66

ization of the core energies and thus to an overall compression (or dilatation) of the odd-A nucleus spectrum.

The experimental and calculated energy levels are compared in Fig. 5. The assignments of the calculated levels to experimental ones is made by considering many different observables (see discussion below). With very few exceptions, the energies and ordering of the known levels is correctly reproduced by the calculations. One should note that the particular pattern of the $\pi=+$ states, such as the low-lying $5/2_1^+$ and $7/2_1^+$ states and the closely packed $13/2^+$, $11/2^+$ and $15/2^+$,$17/2^+$ doublets would have required parameters widely different from those used for the

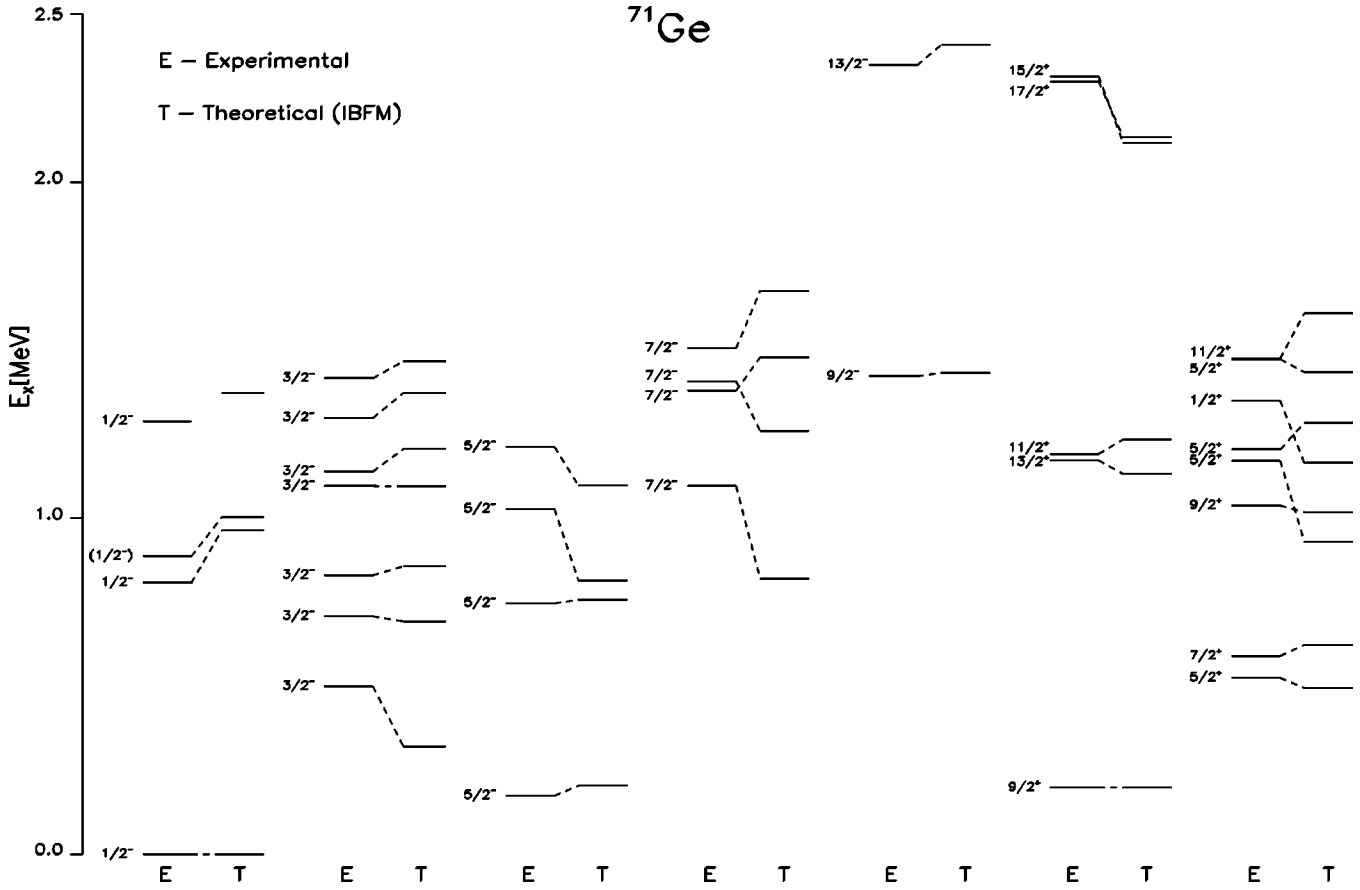

FIG. 5. Comparison between the experimental level scheme of ^{71}Ge and the one calculated with the IBFM-1. Double spin values are given. The dashed lines indicate correspondences between the calculated levels and the experimental ones. For details see text and Tables IV, V, and VI.

$\pi=-$ states if blocking were not considered for the $g_{9/2}$ orbital. Another remark is that ^{71}Ge can be also regarded as a neutron hole coupled to the ^{72}Ge core (which has the same number of bosons with ^{70}Ge, $N=7$). By choosing this core (as calculated in Ref. [18]) and keeping the same *B-F* parameters as above, we have obtained a very similar description.

For the electromagnetic transition operators, besides the parameter values taken from the core nucleus we have used an effective fermion charge $e_F=e_B$, and standard gyromagnetic factors $g_l=0$ and $g_s=-2.68\ \mu_N$ (quenching of 0.7 of the free nucleon value). We have also calculated neutron transfer spectroscopic factors for the theoretical levels. These calculations, performed with the code SPEC [20], used the transfer operators defined, e.g., in Ref. [31] and did not require additional parameters; only the wave functions of the odd-*A* nucleus levels, and those of the 0^+ g.s. of ^{70}Ge (for the neutron stripping case) or of ^{72}Ge (for the neutron pickup case) were necessary. Tables IV and V give details concerning the electromagnetic decay of the states shown in Fig. 4, whereas Table VI shows the one neutron transfer spectroscopic factors.

A few levels need more detailed comments. Thus, the level at $E_x=886.9$ keV has been populated in the β-decay work [1] and assigned as $(3/2, 5/2^-)$ presumably on the basis of its log ft value of 9.1 [1,10]. On the other hand, its properties look rather similar to those of the $E_x=808$ keV, $1/2^-$ state: it is very weakly populated in the β decay [$\log ft=9.14(8)$, compared to 9.1(3) for the 808 keV state], and has strong branches towards the $1/2_1^-$ and $5/2_1^-$ states. The calculated $1/2_3^-$ state fits reasonably well these γ-decay properties (note that in the β decay this state is weakly populated and consequently its γ branches are determined with rather large errors [10]). On these grounds we tentatively identify this state with the theoretical $1/2_3^-$ state. There is a fourth experimental $1/2^-$ level at $E_x=1288.7$ keV which is well fitted in energy by the calculated $1/2_4^-$ level (at 1373 keV—Fig. 4). However, the association of these two levels can only be very tentative, since the calculated decay of the $1/2_4^-$ level resembles only very qualitatively that of the experimental one: the 1288.7 keV state has the largest branch (100) towards the $3/2_2^-$ state and a second weaker branch (11) towards $3/2_1^-$ [10], whereas the calculated $1/2_4^-$ states has indeed important branches towards the two states (13 and 23, towards the $3/2_1^-$ and $3/2_2^-$ states respectively) but its most important branch is towards the $3/2_3^-$ state. The level at $E_x=1171$ keV was observed only in the (d,p) reaction [9], with an $l=2$ transfer, and very weakly in the (p,d) reaction [8]. On this basis (Table VI), although its γ decay is not known, we assigned it as the $5/2_2^+$ level.

A last level to be discussed is the one at 1454.2 keV, assigned as $(1/2^+)$ [10] or $1/2^+,3/2^-$ or $5/2^-$ [6] which decays only to the $1/2_2^-$ level at 808 keV. This γ-decay pattern does not fit any of the higher calculated $3/2^-$ or $5/2^-$ levels; on the other hand, if we assign it to the calculated $1/2_2^+$ level (at 1.6 MeV), its decay towards positive parity levels is predicted as very improbable: it would decay practically only towards the $5/2_1^+$ level, with a high partial lifetime of about 140 ps. Thus, it is likely that this level can be assigned as the predicted $1/2_2^+$ one, but this assignment is, again, only very tentative.

We have thus considered, in Tables IV–VI and the discussion above all the levels known in ^{71}Ge up to an excitation of 1.5 MeV [10]. One could propose assignments of levels calculated with the IBFM-1 to practically all of them. There are a few more levels up to this excitation energy (and above 0.8 MeV) [10], which were evidenced in the (d,p) reaction studies, but nothing is known about them except the excitation energy, so that no attempt could be made at present to speculate about their possible structure.

An examination of Table IV shows that the main γ-decay modes (branching ratios) of the excited states up to about 1.5 MeV are reasonably well reproduced by the calculations. Even in the few cases when the strongest branch (always normalized to 100) is not correctly predicted, one can see that the main experimental branches are also predicted as strong ones. The decay of the 831.3 keV, $3/2_3^-$ state, assumed an ''intruder'' state in the previous IBFM calculations [1,2] is very well reproduced. In the case of the 1212.5 keV, $5/2_4^-$ state, the second state considered intruder in [1,2], the five strong branches are also reasonably well described.

In Table IV, a direct comparison of calculated and experimental transition probabilities can be easily made only for the pure $E2$ transitions. Table V gives a more detailed comparison for those transitions for which more information (other than branching ratios) is known: mixing ratio (at least) and absolute B values. The absolute values of the mixing ratios is reasonably well predicted and, in most of the cases, the sign is also correct. In general, when the experiments presents two possible δ values the one closer to the calculated value provides more correct $B(E2)$ and $B(M1)$ values. The predicted absolute B values follow the experimental trend well, in most of the cases the deviation between the calculations and experiment being within a factor of 2–3; one should emphasize that this result is obtained with transition operators completely determined from the even-even core data.

Table VI presents a comparison of the experimental and calculated stripping $[(d,p)]$ and pickup $[(p,d)]$ spectroscopic factors. The distribution of the strengths for the $p_{1/2}, p_{3/2}, f_{5/2}, g_{9/2}$ orbitals up to $E_x\sim 1.5$ MeV is rather well reproduced. Only the $d_{5/2}$ orbital strength appears to be strongly underestimated both for stripping and pickup, suggesting that the admixture of this orbital in the structure of the lowest states is too small in the present calculations. Indeed, all positive parity states below 2 MeV excitation are strongly dominated (more than 95%) by the $g_{9/2}$ orbital. In the case of the negative parity states, only the $1/2_1^-$, $3/2_1^-$, and $5/2_1^-$ states are dominated by the $p_{1/2}$ (95%), $p_{3/2}$ (81%), and $d_{5/2}$ (97%) orbitals, respectively. The $1/2_2^-$ and $1/2_3^-$ states have very similar configurations: $21\%p_{1/2}+25\%p_{3/2}+53\%f_{5/2}$ and $21\%p_{1/2}+34\%p_{3/2}+40\%f_{5/2}$, respectively, which thus explains the similar properties of the 808 and 886 keV states discussed above. Generally, all the other excited states have rather mixed configurations, with important con-

TABLE IV. Comparison between the experimental and calculated (IBFM-1) decay properties of states in ^{71}Ge. Calculated branches smaller than 0.5 (relatively to the value 100 for the strongest one) are not given unless the experimental counterparts exist. Spin-parity values in the second column are the adopted values from Ref. [10] (see, however, the comment in the text for the 886.9 keV state); the underlined values are those adopted in Ref. [6]. The third column gives the J^π value and the order number of the calculated level assigned to that state. Since for most of the $E2/M1$ mixed transitions the mixing ratios are either unknown or ambiguous, the *experimental* $B(E2)$ and $B(M1)$ values (when available) are given as if the transitions were pure $E2$ or $M1$, respectively. More detailed information on the transitions with known mixing ratios are given in Table V.

E_x (keV)	$J_i^{\pi a}$	$J_i^{\pi b}$	J_f^π	E_γ (keV)	$B(E2)$ (e^2 fm^4) expt.	$B(E2)$ calc.	$B(M1)$ (nm^2) expt.	$B(M1)$ calc.	Br. ratio (%) expt.	Br. ratio (%) calc.
174.9	$5/2^-$	$5/2_1^-$	$1/2_1^-$	174.9	40.1(11)	17.6			100	100
499.9	$3/2^-$	$3/2_1^-$	$1/2_1^-$	499.9		1.7		0.415	100(1)	100
			$5/2_1^-$	325.0		145		2.2×10^{-3}	0.5(1)	0.2
708.2	$3/2^-$	$3/2_2^-$	$1/2_1^-$	708.2	>272	163	>0.0096	0.132	100(2)	100
			$5/2_1^-$	533.3	>79	95	>0.0016	3.8×10^{-3}	7.0(5)	1.8
			$3/2_1^-$	208.3		0.5		0.213		3.9
747.3	$5/2^-$	$5/2_2^-$	$1/2_1^-$	747.3		146			62(2)	100
			$5/2_1^-$	572.4		217		2.1×10^{-5}	100(2)	39.2
			$3/2_1^-$	247.4		144		5.4×10^{-4}	74(1)	0.7
808.3	$1/2^{(-)}$	$1/2_2^-$	$1/2_1^-$	808.3		0		3.2×10^{-4}	62(5)	9.4
			$5/2_1^-$	633.4		79			100(12)	100
			$3/2_1^-$	308.4		18.9		6.5×10^{-3}	24(5)	34.3
			$3/2_2^-$	100.1		179		0.023		4.1
831.3	$3/2^-$	$3/2_3^-$	$1/2_1^-$	831.3		0.40		0.0139	100(2)	100
			$5/2_1^-$	656.4		13.2		5.1×10^{-4}		3.2
			$3/2_1^-$	331.4		118		8.3×10^{-4}	1.9(10)	0.8
			$3/2_2^-$	123.1		134		0.0322		0.8
886.9	$(3/2^-,$	$1/2_3^-$	$1/2_1^-$	886.9		0		4.4×10^{-4}	63(13)	32.5
	$5/2^-)$		$5/2_1^-$	712.0		33.6			100(25)	45.2
			$3/2_1^-$	387.0		69.6		0.0158		100
			$3/2_2^-$	178.7		4.9		0.0722		43.2
			$3/2_3^-$	55.6		102		0.0964		1.7
1026.6	$5/2^-$	$5/2_3^-$	$1/2_1^-$	1026.6	<90	62.4			36.2(10)	33.8
			$5/2_1^-$	851.7	<141	4.0	<0.007	0.0163	21.0(19)	69.1
			$3/2_1^-$	526.7	<7740	533	<0.135	0.091	100(1)	100
			$3/2_2^-$	318.4		3.7		0.135		29.4
			$5/2_2^-$	279.3	<36350	2.8	<0.199	4.3×10^{-4}	21.6(7)	0.1
			$3/2_3^-$	195.3	<14500	429	<0.039	0.0645	1.0(5)	3.3
1095.5	$3/2^-$	$3/2_4^-$	$1/2_1^-$	1095.5	504(112)	120	0.042(9)	8.6×10^{-4}	100.0(14)	100
			$5/2_1^-$	920.6	89(30)	44.2	0.0053(18)	0.0141	7.4(2)	90.3
			$3/2_1^-$	595.6	212(52)	23.4	0.0053(13)	0.0527	2.0(2)	77.6
			$3/2_2^-$	387.3	274(71)	246	0.0029(7)	0.0401	0.30(4)	17.1
			$5/2_2^-$	348.2	1862(517)	9.6	0.0158(44)	6.0×10^{-3}	1.2(2)	1.8
			$1/2_2^-$	287.2	2114(530)	58.5	0.0123(30)	7.4×10^{-4}	0.52(6)	0.2
			$3/2_3^-$	264.2	1235(675)	15.6	0.0061(33)	0.0658	0.2(1)	8.4
			$1/2_3^-$	208.6		101		0.0423		2.7
			$5/2_3^-$	68.9		6.6		0.546		1.2
1096.1	7/2	$7/2_1^-$	$5/2_1^-$	921.2		534		3.8×10^{-4}	100	100
			$3/2_1^-$	596.2		93.5				2.0
			$5/2_2^-$	348.8		93.5		0.0695		12.0

TABLE IV. (*Continued.*)

E_x (keV)	$J_i^{\pi a}$	$J_i^{\pi b}$	J_f^{π}	E_γ (keV)	$B(E2)$ (e^2 fm^4) expt.	calc.	$B(M1)$ (nm^2) expt.	calc.	Br. ratio (%) expt.	calc.
1139.4	3/2	$3/2_5^-$	$1/2_1^-$	1139.4	58(20)	0.6	0.0053(19)	4.1×10^{-3}	100.0(5)	100
			$5/2_1^-$	964.5	11(4)	0.2	0.0007(3)	2.2×10^{-6}	8.5(2)	0.2
			$3/2_1^-$	639.5	64(23)	17.7	0.0018(6)	3.1×10^{-3}	6.1(3)	15.3
			$3/2_2^-$	431.2	195(69)	39.0	0.0026(9)	4.7×10^{-3}	2.6(1)	6.9
			$5/2_2^-$	392.1	519(186)	1.1×10^{-6}	0.0056(20)	1.7×10^{-4}	4.3(3)	0.2
			$1/2_2^-$	331.1	730(280)	58.3	0.0056(21)	0.0137	2.6(4)	8.4
			$3/2_3^-$	308.1	403(185)	123	0.0027(13)	5.5×10^{-3}	1.0(3)	3.0
			$1/2_3^-$	252.5		109		5.5×10^{-4}		0.3
1212.5	$5/2^{(-)}$	$5/2_4^-$	$1/2_1^-$	1212.5	<49	64.8			85.6(15)	100
			$5/2_1^-$	1037.6	<77	7.4	<0.0058(4)	4.5×10^{-3}	62.1(8)	48.0
			$3/2_1^-$	712.6	<812	0.16	<0.0289	9.8×10^{-3}	100.0(18)	30.0
			$3/2_2^-$	504.3	<2865	35.9	<0.0512	0.0186	53(15)	20.7
			$5/2_2^-$	465.2	<1975	445	<0.0300	3.8×10^{-3}	28.8(5)	9.0
			$1/2_2^-$	404.2		94.0				0.6
			$3/2_3^-$	381.2		69.1		1.7×10^{-3}		1.1
			$5/2_3^-$	185.9		82.4		0.090		4.9
1298.7	$3/2^{(-)}$	$3/2_6^-$	$1/2_1^-$	1298.7	303(66)	9.9	0.0359(78)	2.9×10^{-4}	100(2)	93.1
			$5/2_1^-$	1123.8	10.0(29)	1.4	0.0009(3)	8.1×10^{-4}	1.6(3)	38.6
			$3/2_1^-$	798.8		1.0		2.7×10^{-5}		1.1
			$3/2_2^-$	590.5	2028(704)	38.0	0.0497(173)	3.8×10^{-4}	13(4)	7.8
			$5/2_2^-$	551.4	483(220)	7.0×10^{-8}	0.0103(47)	2.3×10^{-4}	2.2(9)	1.1
			$1/2_2^-$	490.4		34.1		1.6×10^{-3}		7.6
			$3/2_3^-$	467.4		33.8		0.0332		100
			$1/2_3^-$	411.8		42.3		0.0103		21.9
			$5/2_3^-$	272.1		0.8		2.4×10^{-3}		1.4
			$3/2_4^-$	203.2		7.0		0.0282		6.9
			$3/2_5^-$	159.3		382		0.274		32.2
1378.7	$7/2^-$, $\overline{5/2}^+$	$7/2_3^-$	$5/2_1^-$	1203.8		0.1		1.6×10^{-5}		4.4
			$3/2_1^-$	878.8		3.5				12.2
			$5/2_2^-$	631.4		106		1.2×10^{-3}	100	100
			$3/2_3^-$	547.4		83.5				27.5
			$5/2_3^-$	352.1		59.7		3.0×10^{-3}		14.6
			$7/2_1^-$	282.6		3.1		1.9×10^{-3}		4.2
			$5/2_4^-$	166.2		470		7.5×10^{-4}		0.7
1406.6	$5/2^-$, $\overline{7/2}^-$	$7/2_2^-$	$5/2_1^-$	1231.7		17.7		5.5×10^{-3}	100(2)	100
			$3/2_1^-$	906.7		179			64.3(24)	55.6
			$3/2_2^-$	698.4		118			28.6(12)	9.9
			$5/2_2^-$	659.3		311		0.0389	99(4)	99.9
			$3/2_3^-$	575.3		123				3.9
			$5/2_3^-$	380.0		349		0.0453	11.9(24)	19.3
			$3/2_4^-$	311.1		1.9			6.2	≈0
			$7/2_1^-$	310.5		87.2		0.0124		2.8
			$5/2_4^-$	194.1		2.2		0.0602		3.2
1415.9	$1/2^-$, 3/2, $5/2^-$	$3/2_7^-$	$1/2_1^-$	1415.9		5.4		2.0×10^{-4}	100	68.4
			$5/2_1^-$	1241.0		0.5		6.6×10^{-6}	40	2.7
			$3/2_1^-$	916.0		0.9		5.1×10^{-3}	20	100
			$3/2_2^-$	707.7		2.6		1.7×10^{-4}		2.3
			$5/2_2^-$	668.6		0.9		5.4×10^{-4}		4.3
			$1/2_2^-$	607.6		83.3		1.4×10^{-3}		20.0
			$3/2_3^-$	584.6		44.2		3.1×10^{-3}		21.2
			$1/2_3^-$	529.0		31.0		3.3×10^{-4}		3.5

TABLE IV. (*Continued.*)

E_x (keV)	J_i^{π}[a]	J_i^{π}[b]	J_f^{π}	E_γ (keV)	$B(E2)$ (e^2 fm^4) expt.	calc.	$B(M1)$ (nm^2) expt.	calc.	Br. ratio (%) expt.	calc.
			$5/2_3^-$	389.3		29.9		1.2×10^{-5}		0.5
			$3/2_5^-$	276.5		31.2		0.0211		11.3
			$3/2_6^-$	117.2		15.9		0.0904		3.7
1422.0	$9/2^-$	$9/2_2^-$	$5/2_1^-$	1247.1	152(32)	88.8			100(6)	100
			$5/2_2^-$	674.7	770(193)	78.7			23(3)	4.1
			$5/2_3^-$	395.4		362				1.3
			$7/2_1^-$	325.9		514		4.1×10^{-3}		1.5
1506.4	$5/2^-$, $\underline{7/2^-}$	$7/2_4^-$	$5/2_1^-$	1331.5	124(40)	0.34	0.0155(49)	2.7×10^{-4}	100(3)	69.9
			$3/2_1^-$	1006.5	277(88)	2.7			55(2)	18.2
			$3/2_2^-$	798.2	468(150)	17.5			29.2(21)	37.7
			$5/2_2^-$	759.1	388(128)	7.0	0.0157(52)	2.1×10^{-3}	18.8(21)	100
			$3/2_3^-$	675.1	270(93)	24.6			7.3(10)	22.9
			$5/2_3^-$	479.8		3.8		0.001		11.1
			$3/2_4^-$	410.9		33.8				2.6
			$7/2_1^-$	410.3		1.1		3.1×10^{-3}		20.5
			$5/2_4^-$	293.9		125		1.2×10^{-4}		2.1
			$7/2_3^-$	127.7		49.7		0.090		17.8
2348.8	$13/2^-$	$13/2_1^-$	$9/2_2^-$	926.8		654			100	100
525.1	$5/2^+$	$5/2_1^+$	$9/2_1^+$	326.7		554			100	100
589.8	$7/2^+$	$7/2_1^+$	$9/2_1^+$	391.4		417		0.0307	100.0(8)	100
			$5/2_1^+$	64.7		354		0.121	<0.7	1.6
1038.2	$9/2^+$	$9/2_2^+$	$9/2_1^+$	839.8		19.6		8.6×10^{-4}	35(15)	53.4
			$5/2_1^+$	513.1		285				34.9
			$7/2_1^+$	448.4		212		0.0196	100(50)	100
1171	$5/2^+$	$5/2_2^+$	$9/2_1^+$	973		41.2				10.1
			$5/2_1^+$	646		339		2.2×10^{-3}		13.1
			$7/2_1^+$	581		388		0.118		100
1172.4	$13/2^+$	$13/2_1^+$	$9/2_1^+$	974.0	735(140)	504			100	100
1192.3	$11/2^+$	$11/2_1^+$	$9/2_1^+$	993.9	633(127)	136	0.044(9)	0.0130	100	100
			$7/2_1^+$	602.5		526				13.3
1205.1	$5/2^+$	$5/2_3^+$	$9/2_1^+$	1006.7		0.5				0.6
			$5/2_1^+$	680.0	538(136)	135	0.0175(44)	2.4×10^{-3}	18.4(8)	25.7
			$7/2_1^+$	615.3	4820(1210)	77.3	0.1282(322)	0.0497	100.0(6)	100
1349.0	$1/2^+$	$1/2_1^+$	$5/2_1^+$	823.9	637(153)	667			100	100
1474	$(5/2)^+$	$5/2_4^+$	$9/2_1^+$	1276		4.3				31.7
			$5/2_1^+$	949		2.7		7.6×10^{-4}		24.8
			$7/2_1^+$	884		30.3		2.7×10^{-3}	100	100
			$9/2_2^+$	436		170				5.8
			$5/2_2^+$	303		166		0.0514		45.3
			$5/2_3^+$	269		203		0.0384		23.8
1477.0	$11/2^+$	$11/2_2^+$	$9/2_1^+$	1278.6	166(31)	156	0.0176(36)	4.2×10^{-3}	100(9)	100
			$7/2_1^+$	887.2	820(170)	5.8			86(6)	0.5
			$13/2_1^+$	304.6		3×10^{-8}		0.0129		0.8
2298.7	$17/2^{(+)}$	$17/2_1^+$	$13/2_1^+$	1126.3		911			100	100
2314.2	$15/2^{(+)}$	$15/2_1^+$	$13/2_1^+$	1141.8		85.5		0.0113	70(30)	27.5
			$11/2_1^+$	1121.9		829			100(14)	100
			$11/2_2^+$	837.2		113				3.2

[a]Adopted values from ENSDF (Ref. [10]); underlined values have been proposed in Ref. [6];
[b]Assigned values (comparison with the IBFM calculations).

TABLE V. Comparison between calculated and experimental $B(E2)$, $B(M1)$ and $\delta(E2/M1)$ values. Included here are only the mixed transitions for which at least the δ value has been measured. For the δ values we quote either the adopted values [10], or more recent results; in some cases the values from Ref. [7] are given. In many cases two possible values were given for the experimental δ and, when the lifetime of the state is available, we give $B(\sigma L)$ values corresponding to both values. Generally, the theoretical values are placed on the same line with the experimental values for which the agreement appears to be better.

						$B(E2)$ (e^2 fm^4)		$B(M1)$ (nm^2)	
E_x (keV)	J_i^π	J_f^π	E_γ (keV)	$\delta_{\rm exp}$	$\delta_{\rm IBFM}$	expt.	calc.	expt.	calc.
499.9	$3/2_1^-$	$1/2_1^-$	499.9	$+0.11(2)$[b]	$+0.009$		1.7		0.415
				or $-2.3(1)$					
708.2[a]	$3/2_2^-$	$1/2_1^-$	708.2	$-2.90^{+0.76}_{-1.40}$[e]		$>250(20)$		$>0.0010(3)$	
				or 0.19(9)	$+0.22$	$>10(9)$	163	$>0.009(2)$	0.132
747.3	$5/2_2^-$	$5/2_1^-$	572.4	$-0.07(7)$[b]	-15.5		217		2.1×10^{-5}
		$3/2_1^-$	247.3	$-2.14^{+0.34}_{-0.47}$[e]	-1.07		144		5.4×10^{-4}
				or $-0.18(7)$					
1026.6[a]	$5/2_3^-$	$1/2_1^-$	1026.6	E2		<90	62.4		
		$5/2_1^-$	851.7	$0.0^{+3.2}_{-0.26}$[c]	$+0.11$	<128	4.0	<0.007	0.0163
		$3/2_1^-$	526.7	$-0.16(3)$[c]	-0.34	<233	533	<0.138	0.091
		$5/2_2^-$	279.3	$-0.12^{+0.17}_{-0.19}$[e]	$+0.19$	<1980	2.8	<0.258	4.3×10^{-4}
				or $2.48^{+2.22}_{-0.84}$		<34000		<0.036	
1095.5[a]	$3/2_4^-$	$1/2_1^-$	1095.5	$-3.2(2)$[c]	$+3.41$	458(102)	120	0.0038(9)	8.7×10^{-4}
				or $+0.23$		25(6)		0.040(9)	
		$5/2_1^-$	920.6	$\geqslant 3.7$[c]		>55		$<3.6\times10^{-4}$	
				or $+0.36(14)$	$+0.43$	10.2(74)	44.2	0.0047(16)	0.0141
1096.0	$7/2_1^-$	$5/2_1^-$	921.1	$-2.99(44)$[d]	$+28.9$		534		3.7×10^{-5}
				or $-0.10(7)$					
1139.4[a]	$3/2_5^-$	$1/2_1^-$	1139.4	$-0.45(5)$[c]	$+0.11$	9.8(39)	0.6	0.0044(16)	4.1×10^{-3}
				or $-6.8(14)$		57(20)		$1.1(4)\times10^{-4}$	
		$5/2_2^-$	392.1	$0.06\div0.09$[c]	$+0.008$	$7(3)\times10^{-4}$	0.15	0.0014	2.1×10^{-6}
				or $-4.3^{+1.7}_{-1.1}$		10.8(38)		$3.8(15)\times10^{-5}$	
1212.5[a]	$5/2_4^-$	$1/2_1^-$	1212.5	E2		<24	64.8		
		$5/2_1^-$	1037.6	$-0.10(6)$[c]		<2.0		<0.007	
				or 2.1(3)	$+0.35$	<76	7.4	<0.0014	4.6×10^{-3}
		$3/2_1^-$	712.6	$-0.19^{+0.11}_{-0.09}$[c]	-0.024	<64	0.16	<0.038	0.010
				or $-1.8^{+0.5}_{-0.4}$		<798		<0.0096	
		$3/2_2^-$	504.3	$0.31^{+0.27}_{-0.24}$[e]	$+0.19$	<595	35.9	<0.067	0.0186
1298.7[a]	$3/2_6^-$	$1/2_1^-$	1298.7	0.04(3)[c]		0.5(7)		0.036(8)	
				or $-1.88(11)$	-2.01	236(51)	9.9	0.0079(18)	2.9×10^{-4}
1406.7	$7/2_1^-$	$5/2_1^-$	1231.8	$+0.58(15)$[d]	$+0.58$		17.7		0.0056
				or $+3.15(44)$					
589.8	$7/2_1^+$	$9/2_1^+$	391.4	$-0.23(4)$[b]	-0.38		417		0.0307
1038.2	$9/2_2^+$	$9/2_1^+$	839.8	$+0.4^{+0.1}_{-0.3}$[b]	-1.05		19.6		8.7×10^{-4}
		$7/2_1^+$	448.4	$+0.49(6)$[b]	-0.39		212		0.0196
1192.3	$11/2_1^+$	$9/2_1^+$	993.9	$+1.3(2)$[b]	$+0.85$	398(92)	136	0.0163(40)	0.0130
1205.1[a]	$5/2_3^+$	$5/2_1^+$	680.0	$0.07^{+0.33}_{-0.25}$[e]		2.6(22.3)		0.017(11)	
				or $1.15^{+1.33}_{-0.64}$	$+1.36$	305(220)	135	0.0075(61)	0.0024
		$7/2_1^+$	615.3	$-2.6^{+0.7}_{-0.5}$[c]		4190(1080)		0.0165(49)	
				or $-0.23(9)$	-0.20	242(170)	77.3	0.121(36)	0.0497
1477.0	$11/2_2^+$	$9/2_1^+$	1278.6	$+4.7(8)$[b]	$+2.07$	159(32)	156	$8^{+6}_{-3}\times10^{-4}$	0.0042

[a]Lifetime (or limit) determined in present work.
[b]Adopted value [10].
[c]Reference [2].
[d]Present work.
[e]Malan *et al.* [7].

TABLE VI. Comparison between experimental and calculated one neutron transfer spectroscopic factors (C^2S).

E_x (MeV)	J^π	(d,p)[a]		(p,d)[b]	
		expt.	IBFM	expt.	IBFM
0.0	$1/2_1^-$	0.62	0.82	0.86	1.17
0.500	$3/2_1^-$	0.36	0.49	1.61	2.22
0.708	$3/2_2^-$	$\leqslant$0.07	0.14	0.14	0.73
0.831	$3/2_3^-$		0.02	0.01	0.19
1.096	$3/2_4^-$	0.14	0.004	0.29	0.004
0.175	$5/2_1^-$	1.49	1.39	3.72	4.03
0.747	$5/2_2^-$	0.12	0.06	0.38	0.20
1.027	$5/2_3^-$		0.03	0.16	0.13
1.212	$5/2_4^-$		0.0005	0.19	0.04
0.198	$9/2_1^+$	4.15	6.30	1.97	1.79
0.525	$5/2_1^+$	0.52	0.23	0.18	0.0005
1.171	$(5/2_2^+)$	0.78	0.05		0.0
1.205	$5/2_3^+$	0.32	0.003		0.0
1.474	$5/2_4^+$	0.11	0.04		0.0

[a]Reference [9].
[b]Reference [8].

tributions from the orbitals $p_{1/2}$, $p_{3/2}$, and $f_{5/2}$ and very small contribution from the $f_{7/2}$ orbital.

V. CONCLUSIONS

In the present work we have reported the first measurements of lifetimes of excited states in ^{71}Ge in the picosecond region with the DSA method in the $(p,n\gamma)$ reaction. Lifetimes (or lower limits) could be determined for twelve states with excitation energy below 2.0 MeV and low spin values (up to 7/2).

The structure of this nucleus has been investigated within the interacting boson-fermion model. A reinvestigation of the core nucleus ^{70}Ge based on all presently available experimental data, has shown that up to about 3.0 MeV excitation its properties are well described by the IBM model. Using this core, both the negative and the positive parity states in ^{71}Ge have been reasonably described with the *same* set of IBFM parameters, essential for this being the blocking of the unique parity orbital $g_{9/2}$. Assignments of the experimental levels to the calculated ones have been made on the basis of all existing experimental data, including excitation energies, J^π values, γ-decay branching ratios, mixing ratios, absolute γ-ray transition probabilities, and one neutron transfer spectroscopic factors. The calculations account well for the properties of the experimental levels of low spin known in this nucleus up to about 1.5 MeV, and the higher spin yrast states below 2.5 MeV. Thus, all levels in ^{71}Ge up to 1.5 MeV can be rather satisfactorily explained by the coupling of the odd particle occupying the valence shell orbitals to collective excitations of the core. Other excitation modes may be present at higher energies, where, however, more complete experimental data are still required both quantitatively and qualitatively.

ACKNOWLEDGMENT

This work was partly supported by a research grant from the Romanian Ministery for Science and Technology.

[1] R.A. Meyer, R.J. Nagle, S. Brant, E. Frlez, V. Paar, and P.K. Hopke, Phys. Rev. C **41**, 686 (1990).
[2] W.D. Hamilton, W.L. Croft, W.H. Brantley, L.A. Rayburn, I.C. Girit, S. Brant, and V. Paar, Phys. Rev. C **47**, 1042 (1993).
[3] K. Forssten, A. Hasselgren, P. Monseu, A. Nilsson, and Z.P. Sawa, Phys. Scr. **10**, 51 (1974).
[4] U. Eberth, J. Eberth, E. Eube, and V. Zobel, Nucl. Phys. **A257**, 285 (1976).
[5] D.T. Kelly, P.W. Green, and J.A. Kuchner, Nucl. Phys. **A289**, 61 (1977).
[6] D. Fedorets, I.I. Zalyubovskii, V.E. Mitroshin, B.A. Nemashkalo, and S.S. Ratkevitch, Phys. At. Nucl. **56**, 436 (1993).
[7] J.G. Malan, E. Barnard, J.A.M. de Villiers, and P. van der Merwe, Nucl. Phys. **A227**, 399 (1974).
[8] R. Fournier, J. Kroon, T.H. Shu, and B. Hird, Nucl. Phys. **A202**, 1 (1973).
[9] J.A. Bieszk, L. Montestruque, and S.E. Darden, Phys. Rev. C **16**, 1333 (1977).
[10] M.R. Bhat, Nucl. Data Sheets **68**, 579 (1993).
[11] F. Iachello and O. Scholten, Phys. Rev. Lett. **43**, 679 (1979).
[12] J. Lindhard, M. Scharff, and H.E. Schiott, Mat. Fys. Medd. Dan. Vid. Selsk. **33**, (1963).
[13] A. Blaugrund, Nucl. Phys. **88**, 501 (1966).
[14] A.A. Alexandrov, M.P. Kudoyarov, I.Kh. Lemberg, and A.A. Pasternak, Nucl. Phys. **A321**, 189 (1979).
[15] G. Audi, O. Bersillon, J. Blachot, and A. Wapstra, Nucl. Phys. **A624**, 1 (1997).
[16] J.F. Ziegler, computer code TRIM, 1992, presented in J.F. Ziegler, J.P. Biersack, and U. Littmark, *The Stopping and Range of Ions in Solids* (Pergamon Press, New York, 1985)
[17] T. Yamazaki, Nucl. Data, Sect. A **3**, 1 (1967).
[18] D. Bucurescu, I. Cătа-Danil, M. Ivaşcu, N. Mărginean, L. Stroe, C.A. Ur, and N. Dinu, Int. J. Mod. Phys. E (to be published).
[19] O. Scholten, computer codes ODDA and PBEM, KVI Internal Report No. 252, 1982.
[20] O. Scholten, computer code SPEC (unpublished).
[21] A. Arima and F. Iachello, Ann. Phys. (N.Y.) **99**, 253 (1976); **111**, 201 (1978); Phys. Rev. Lett. **40**, 385 (1978).
[22] F. Iachello and A. Arima, *The Interacting Boson Model* (Cambridge University Press, Cambridge, 1987).
[23] M.R. Bhat, Nucl. Data Sheets **68**, 117 (1993).
[24] O. Scholten, Computer codes PHINT and FBEM, KVI Report No. 63, 1979.
[25] P.O. Lipas, P. Toivonen, and D.D. Warner, Phys. Lett. **155B**, 295 (1985).

[26] W.-T. Chou, N.V. Zamfir, and R.F. Casten, Phys. Rev. C **56**, 829 (1997).
[27] P.O. Lipas, E. Hammaren, and P. Toivonen, Phys. Lett. **139B**, 10 (1984).
[28] P.O. Lipas, P. Toivonen, and E. Hammaren, Nucl. Phys. **A469**, 348 (1987).
[29] R. Bijker and A.E.L. Dieperink, Nucl. Phys. **A379**, 221 (1982); R. Bijker and O. Scholten, Phys. Rev. C **32**, 591 (1985).
[30] B.S. Reehal and R.A. Sorensen, Phys. Rev. C **2**, 819 (1970).
[31] O. Scholten and T. Ozzello, Nucl. Phys. **A424**, 221 (1984).